Mesoporous Materials

DOI: 10.1002/ange.201301766

Gel-Free Secondary Growth of Uniformly Oriented Silica MFI Zeolite Films and Application for Xylene Separation**

*Tung Cao Thanh Pham, Thanh Huu Nguyen, and Kyung Byung Yoon**

Continuous zeolite films grown on porous supports[1–15] bear great potential to replace the current energy-inefficient distillation-based separation methods.[14,15] For their successful applications in industry, they should be grown by satisfying the following requirements. The first is to grow them with the channels vertically oriented with respect to the substrate planes from the top to the bottom of the films to maximize the permeance. The second is to grow them as thin as possible also to maximize the permeance. The third is to grow them pinhole-free to maximize the separation factor. The fourth is to grow them so that they do not form cracks during calcination to remove organic templates for those template bearing zeolite films. The fifth is to grow them economically by saving chemicals, simplifying procedures, and replacing expensive porous alumina supports with less expensive ones. The sixth is to grow them environment-friendly by not producing any wastes. However, despite the great efforts that have been made in this field, there have not been such methods that satisfy all of the above requirements.

Silicalite-1 (SL) is a pure silica MFI[16] zeolite with 5.5 × 5.1 Å sized elliptical channels running along the *a* axis in a sinusoidal manner and 5.6 × 5.3 Å sized elliptical channels running straight along the *b* axis (Figure 1 a).[17] The growth of SL films traditionally begins with the preparation of appropriate gels by mixing a Si source, tetrapropylammonium hydroxide (TPAOH), and water, followed by aging the gels for desired periods of time. Usually seeded porous alumina substrates are immersed into the gels and they are subsequently heated for desired periods of time in a Teflon-lined autoclave. After their growth, the films are removed from mother liquors, washed with copious amounts of water, and dried in an oven. A majority of the gel is converted to unwanted SL powders, and the remaining highly basic TPAOH-containing mother liquors should be disposed after neutralization with an acid such as hydrochloric acid. In fact, the produced tetrapropylammonium chloride should be removed from the waste water before disposal. Also, large amounts of water used for washing the films are disposed into the drains.

Furthermore, even with the substrates coated with closely packed monolayers of *a*- or *b*-oriented SL crystals, the produced SL films became randomly oriented. Because of this, the films should be grown thick until the gaps between the randomly oriented SL crystals disappear. The produced randomly oriented SL films also have a great tendency to undergo crack formation during calcination to remove the entrapped tetrapropylammonium ions.

Recently, we reported a novel method which satisfies the first four requirements.[18] However, this method still needs a gel preparation step, and not all of the gel is converted to the films from the practical point of view, and hence some of the gel should eventually be discarded. The produced films should also be washed with copious amounts of water. Thus, the method still does not satisfy the last two requirements.

In fact, the use of gels for the growth of films has been the common tradition in this field. Because of this, extra time and large amounts of chemicals have been wasted. Now, if there is a gel-free yet facile method that satisfies the first four requirements, this method would be revolutionary because this method automatically satisfies even the last two requirements. Then the procedure becomes much simpler, saves time, does not need the gel preparation step, gel aging step, washing of the films and reactors, drying of the films, and neutralization of mother liquors for disposal, the recovery of organic salts from the neutralized mother liquors, and the disposal of unreacted gels, mother liquors, neutralizing acids, organic salts, and large amounts of water used for film washing is not necessary.

In 2007, Okubo and co-workers reported a novel method of growing SL films on a Si wafer by merely coating a Si wafer with 1M TPAOH solution followed by treating the TPAOH-coated Si wafer with steam in an autoclave.[19] The native or intentionally produced oxide layer on the surface of the Si wafer acted as the Si source, TPAOH acted as both the base and the structure-directing agent, and water was supplied from the steam. This method is different from steam-assisted growths of SL films from gel-coated substrates.[20,21] In this regard, this method can be named as gel-free growth of SL films on a substrate, in particular, as gel-free primary growth because no seed crystals were used.[22] However, the orientations of the produced SL films became random (Figures S1 and S2 in the Supporting Information). Accordingly, the film should be grown thick (> 2 μm) to cover the whole substrate with the film. Sankar and co-workers also recently reported

[*] Dr. T. C. T. Pham, T. H. Nguyen, Prof. Dr. K. B. Yoon
Korea Center for Artificial Photosynthesis
Center for Microcrystal Assembly
Department of Chemistry, Sogang University
Seoul 121-742 (Korea)
E-mail: yoonkb@sogang.ac.kr

[**] This work was supported by the Korea Center for Artificial Photosynthesis (KCAP) located in Sogang University funded by MSIP through the National Research Foundation of Korea (grant number 2012M1A2A2671784 and grant number 2012R1A2A3A01009806). We thank Yonsei-Carl Zeiss Advanced Imaging Center for LSCM measurements, KBSI (Daejeon) for Focused Ion Beam (FIB) cutting, and Jiyun Lee for the help in drawing Figures 1 and 2.

Supporting information for this article is available on the WWW under http://dx.doi.org/10.1002/anie.201301766.

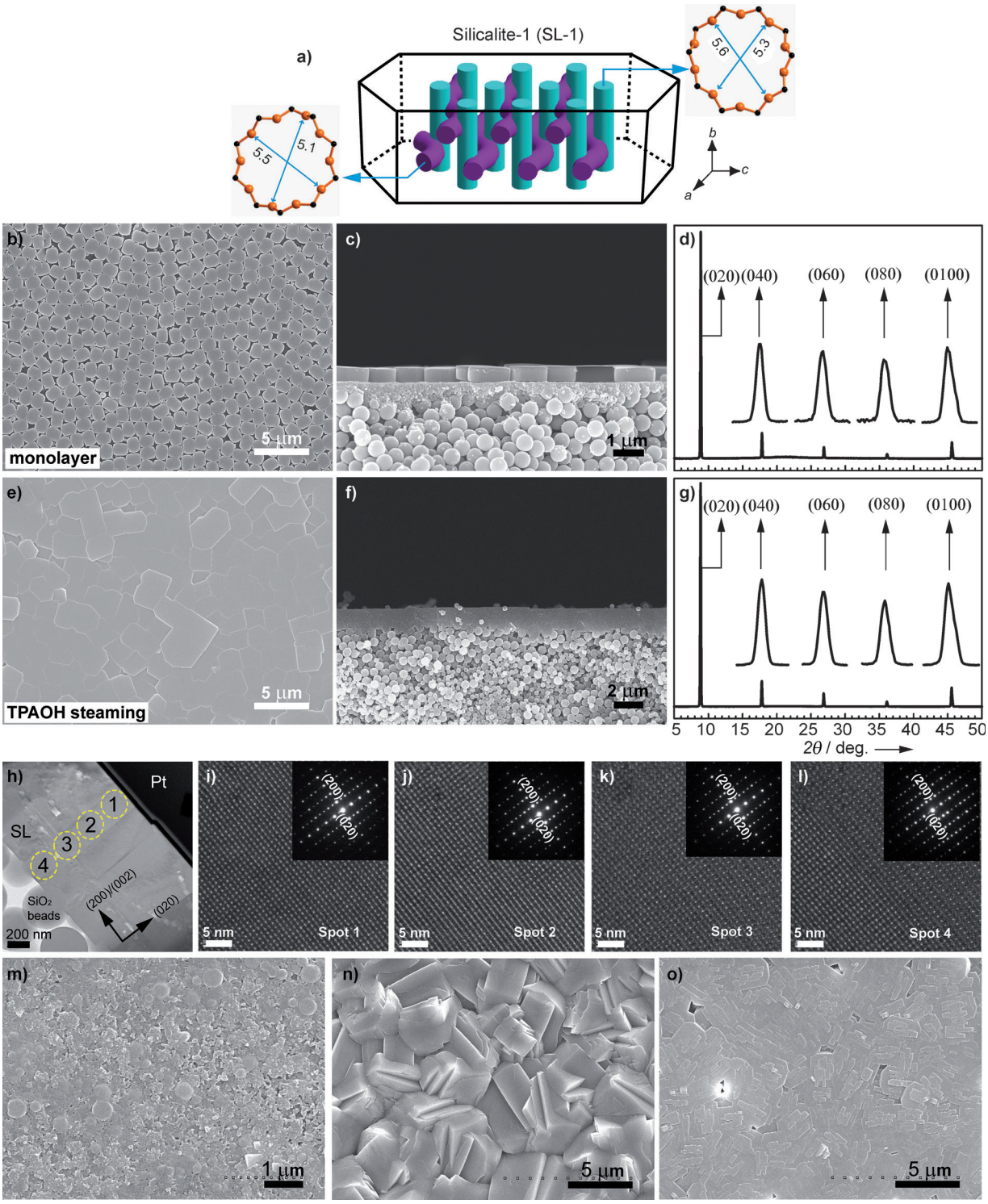

Figure 1. a) A coffin-shaped SL crystal and its channel systems. b–d) Top and side view SEM pictures and X-ray diffraction pattern of a monolayer of *b*-oriented SL crystals assembled on a silica bead support. e–g) A uniformly *b*-oriented continuous SL film supported on a silica bead support. h) TEM picture of a piece of a uniformly *b*-oriented SL film grown on a silica bead support prepared by a focused ion beam cutter and mounted to a copper TEM grid with Pt as the glue. i–l) Lattice pictures and the selected area electron diffraction patterns of the four spots in (h). m,n) Top view SEM pictures of *d*-SiO_2 supports after gel-free primary growth processes using 0.05 (m) and 1 M (n) TPAOH solutions, for 48 and 12 h, respectively. o) Top view SEM picture of a continuous SL film produced by gel-free secondary growth for 6 h using a 1 M TPAOH solution, showing the appearance of *a*, *b*, and other orientations.

the production of randomly oriented SL and Ti-doped SL films on silicon wafer and alumina by applying this method.[23]

Thus, despite of its importance, gel-free primary growth has not been widely used nor developed into practically useful methods. We now report an unprecedented gel-free secondary growth that reproducibly satisfies all of the aforementioned six requirements. We furthermore demonstrate application of the *b*-oriented SL membranes for the separation of a mixture of *ortho*- and *para*-xylenes.[4–8]

We first prepared porous silica (p-SiO_2) disks with a diameter of 20 mm and thickness of 3 mm using a mixture of 350 and 550 nm sized silica beads according to the reported procedure (see the Methods Section in the Supporting Information).[18] On one face of each p-SiO_2 disk a layer of 50 nm silica beads was coated with the thicknesses of about 200 nm to make the surface smoother. The overall procedure to prepare p-SiO_2 disks requires less amounts of energy and time than those of porous alumina supports because sintering of the amorphous silica beads into the disk-shaped supports requires a lower temperature (1020 °C) and shorter period of time (2 h) than those of crystalline alumina powder (800 °C, 24 h and 1240 °C, 2 h) into porous supports (see the Methods Section in the Supporting Information). Rounded coffin-shaped SL crystals with the size of $1.5 \times 0.6 \times 1.9\ \mu m^3$ were also prepared (see the Methods Section and Figure S3 in the Supporting Information). These were assembled into uniformly *b*-oriented monolayers [$(b\text{-SL})_m$] on the smoother side of p-SiO_2 disks by rubbing[18,24,25] (see the Methods Section in the Supporting Information), as demonstrated by the top (Figure 1 b) and side view (Figure 1 c) scanning electron microscopy (SEM) of a film. The X-ray diffraction pattern of the film (Figure 1 d) only shows the diffraction peaks from the (020), (040), (060), (080), and (0100) planes.

The $(b\text{-SL})_m$-coated p-SiO_2 disk [$(b\text{-SL})_m/p$-SiO_2-disk] was partially wetted with a dilute (0.025 M) TPAOH solution by dipping a half of the disk with the $(b\text{-SL})_m$ side facing down into the TPAOH solution for 40 s, followed by drying the disk for 5 s in the atmosphere. The TPAOH-coated $(b\text{-SL})_m/p$-SiO_2-disk plate was placed horizontally with the $(b\text{-SL})_m$ side pointing upward at the bottom of a clean Teflon-lined autoclave (volume = 25 mL) and the sealed autoclave was placed in a preheated (190 °C) oven for varying periods of time between 5 and 50 h (see the Methods Section in the Supporting Information). The *b*-SL crystals become interconnected and the intercrystalline gap disappeared with time, giving rise to the formation of a perfectly *b*-oriented continuous SL film, as demonstrated by the top (Figure 1 e) and side view (Figure 1 f) SEM pictures of a film grown for 12 h. The X-ray diffraction pattern of the film (Figure 1 g) shows only the diffraction peaks from the (020), (040), (060), (080), and (0100) planes, confirming that the film is indeed perfectly *b*-oriented. The lattice fringes and the selected-area electron diffraction patterns of the cross-sections of the films are identical regardless of the depth within the film (Figure 1 h–l), confirming once again that the SL films grow in perfect *b*-orientation regardless of the film depth.

For comparison, we also conducted gel-free primary growth of SL films on bare p-SiO_2 disks. Interestingly, when the TPAOH concentration was low ($\leq$ 0.05 M) the gel-free primary growth did not take place even after 48 h (Figure 1 m), indicating that at TPAOH concentrations lower than 0.05 M the formation of SL crystals does not take place. This phenomenon is contrasted with our gel-free secondary growth by which the SL film grows very readily. Thus, under the low TPAOH condition, gel-free primary growth does not take place whereas the gel-free secondary growth takes place readily. This is a very interesting phenomenon that occurs only under the gel-free growth condition (but not under the gel-based condition) and this phenomenon is a key to the success to the downward growth of uniformly *b*-oriented SL films. Otherwise, randomly oriented SL films would be produced. In that sense, the low TPAOH concentration is likened to TEAOH, which acted as the suppressor of the autogenesis of SL crystals in the bulk medium gel, giving rise to only the upward growth of uniformly *b*-oriented SL films during gel-based secondary growth.[18]

Indeed, at the TPAOH concentration of 1 M, randomly oriented SL films readily grew on p-SiO_2 disks under the gel-free primary condition (Figure 1 n and Figure S4), indicating that the formation of SL crystals takes place when the TPAOH concentration is high. Consistent with this, when the gel-free secondary growth was carried out with 1 M TPAOH solution (or when the concentration is larger than 0.2 M) the produced SL film became randomly oriented (Figure 1 o and Figures S5 and S6), confirming that both the presence of *b*-oriented SL seed crystals and the use of a low TPAOH concentration are crucial to the success of gel-free secondary growth. Of course, a randomly oriented SL film was formed on a $(b\text{-SL})_m/p$-SiO_2-disk when gel-based secondary growth was conducted using a conventional TPAOH gel (Figure S7).

Under our gel-free secondary growth condition, the Si source for the newly grown SL layer is primarily supplied from the 50 nm sized SiO_2 beads as evidenced by their gradual disappearance with time as the intercrystalline gaps disappear and the film thickness increases as the top (Figure 2 a–c) and side (Figure 2 d–f) view SEM pictures show. The cross-sectional transmission electron microscope (TEM) picture (Figure 2 g) revealed that the new SL layer grows mostly downwards towards the underlying silica supports from the bottom of the seed SL crystals. Although small, the upward film growth also takes place. This indicates that small amounts of Si source and TPAOH are transported from the bottom to the top of the film. Considering the small amount of moisture adsorbed in the support (about 0.5 g) and the large volume of the autoclave (25 mL), the upward transport of the Si source and TPAOH from the bottom to the top of the film is attributed to the in situ formation of a TPAOH gel and the subsequent upward movement of the gel by the capillary force along the crystal gaps and surface adhesion force. Because of the simultaneously undergoing upward film growth along the *b*-axis the upper film surface becomes smoother.

The consumption of the underlying 50 nm silica beads leads to a direct connection between the lower part of the film and the top of the 350/550 nm SiO_2 bead layer (Figure 2 g). The seed crystals grow faster along the *c* and *a* axes than along the *b* axis, giving rise to the formation of continuous SL films. The brief mechanism is illustrated in Figure 2 h. As indicated in this scheme (bottom part of Figure 2 h), and as shown in

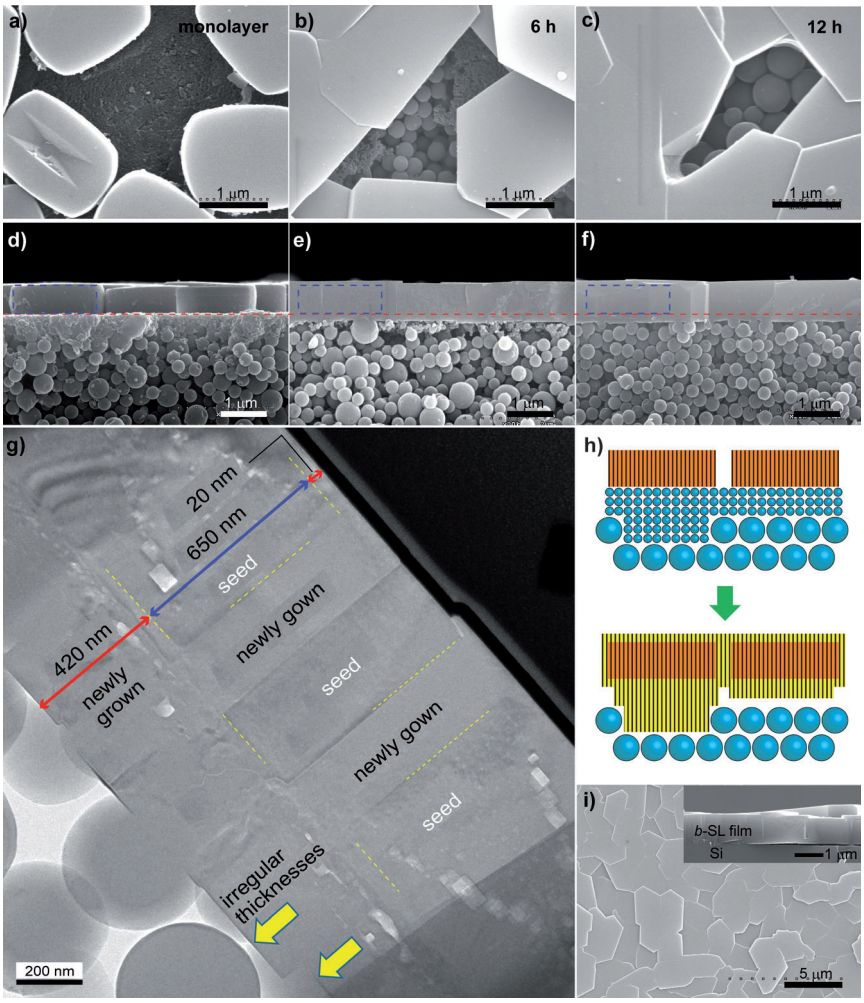

Figure 2. Top (a–c) and side (d–f) view SEM pictures of *b*-oriented monolayers of SL crystals assembled on a 550 nm silica bead support coated with a 200 nm thick layer of 50 nm silica beads before (a,d) and after gel-free secondary growth for 6 (b,e) and 12 h (c,f). g) An enlarged TEM picture f) showing the initial SL seed and newly grown sections and the irregular depths. h) The growth mechanism. i) Top and side (inset) view SEM pictures of a *b*-oriented SL film grown on a Si wafer which had a 200 nm thick amorphous silica layer on the surface.

Figure 2g (at the left bottom), the *b*-oriented film becomes partially self-supporting. This will help increase the permeances of the films during their applications as molecular sieve membranes. The gel-free secondary growth of *b*-oriented SL films also works well on Si wafers coated with an amorphous silica layer, on fused silica plates, and on F-doped tin oxide (FTO) glass, as a top view SEM picture shows for the case of a Si wafer (Figure 2i). This method thus can be applied for the preparation of uniformly oriented SL films on various substrates for various applications.[26–33]

We applied the laser scan confocal microscope (LSCM), a method developed by the research group of Tsapatsis,[34] as a means to analyze the cracks in SL films. The randomly oriented SL films (Figure 3a) readily underwent crack formation upon calcination at 500 °C, as two- (2D; Figure 3b) and three-dimensional (3D; Figure 3c) LSCM pictures of the fluorescein-treated SL film show. In contrast, the perfectly *b*-oriented SL films never showed cracks (Figure 3d) despite the fact that the SL films have many regions which are self-supporting. Accordingly, special thermal annealing[4] was not necessary to prevent the formation of cracks.

To investigate the performance of uniformly *b*-oriented SL films, we prepared two uniformly *b*-oriented SL membranes with two different thicknesses, 1000 and 200 nm (see the Methods Section and Figure S8 in the Supporting Information). The separation of the *o*- and *p*-xylene mixture was conducted at two different temperatures (150 and 200 °C) under standard conditions (see the Methods Section in the Supporting Information). In the case of the 1000 nm thick membrane, the initially measured permeance of *p*-xylene at 150 °C was 23×10^{-8} mol s^{-1} m^{-2} Pa^{-1} (Figure 4). This was much higher than that of *o*-xylene, giving rise to a very high initial separation factor (SF > 3000). However, the permeance of *p*-xylene continuously decreased over a period of 480 h without reaching a steady state. Because the decrease in *p*-xylene permeance is caused by the gradual increase in the degree of channel clogging with *o*-xylene,[18] this phenomenon is an indication that the membrane is pinhole- and crack-free. The permeance of *p*-xylene after 480 h was 7.5×10^{-8} mol s^{-1} m^{-2} Pa^{-1}. The SF also continuously decreased until 375 h and reached a steady state of 680 after 375 h.

In the case of the 200 nm thick membrane, the permeances of *p*- and *o*-xylene maintained at 12×10^{-8} and 0.009×10^{-8} mol s^{-1} m^{-2} Pa^{-1}, respectively, over the period of 380 h. The SF reached the steady-state value of 1100 after 50 h, the highest SF value ever obtained from thin SL membranes with the thickness equal to or less than 200 nm. For example the research group of Tsapatsis showed a SF of 483 for a 1000 nm thick SL membrane,[6,8] 139 for a 500 nm thick SL membrane,[4] and 70 for a 200 nm thick film.[14] The two results from our 1000 and 200 nm thick films show that the thinner membrane is much more favorable for higher permeance and SF.

In the case of the 1000 nm thick membrane, the *p*-xylene permeance and SF did not reach the steady state even at 200 °C. In the case of the 200 nm thick film, however, these values very quickly reached the steady states (*p*-xylene permeance = 13×10^{-8} mol s^{-1} m^{-2} Pa^{-1} and SF = 1050), indicating that the channel clogging by *o*-xylene does not occur because of the short channel length. In the case of the 200 nm thick membrane, based on the fact that the SF values are the same (about 1100), the permeance values are similar ($12–13\times10^{-8}$ mol s^{-1} m^{-2} Pa^{-1}) regardless of the temperature (150 or 200 °C), and the film is partially self-supporting and pinhole-

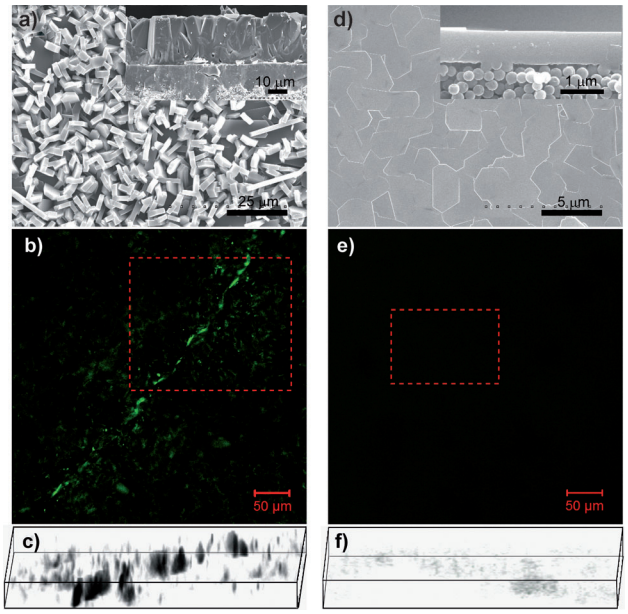

Figure 3. a) Top and side (inset) SEM pictures and b,c) two- (2D) and three-dimensional (3D) LSCM pictures of a calcined, randomly oriented SL membrane after treatment with fluorescin. d) Top and side view (inset) SEM pictures and e,f) 2D and 3D LSCM pictures of a calcined, uniformly *b*-oriented SL membrane after treatment with fluorescin. The 3D pictures were built after caring out slice scans in the selected areas indicated in (b) and (e). Note that the laser wavelength and power (488 nm and 2.6%), zoom value (1.0), and master gain (585) are the same for both cases.

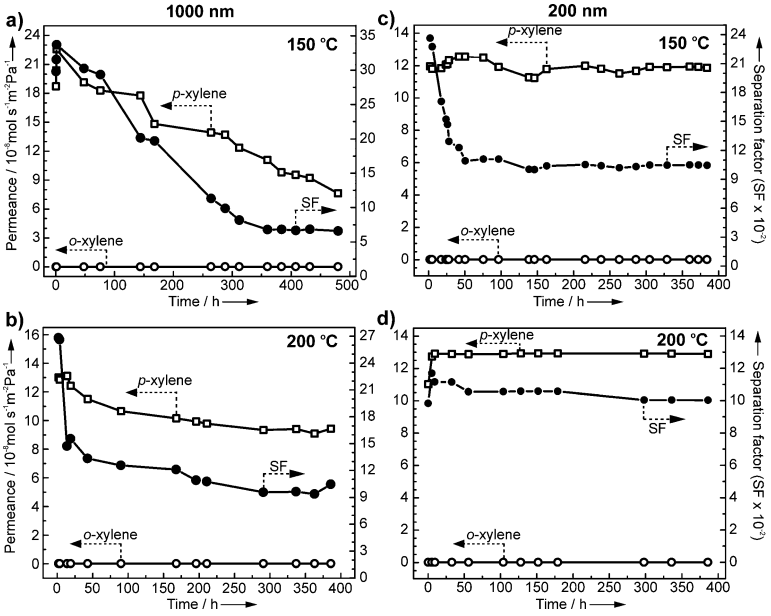

Figure 4. Plots of permeances of *p*- (open square) and *o*-xylene (open circle) and the separation factor (filled circle) with time for the two SL films of two different thicknesses, 1000 (a,b) and 200 nm (c,d) at two operation temperatures, 150 (a,c) and 200 °C (b,d).

free, we propose that they are close to the maximum permeance and SF values that can be reached by an ideal SL membrane.

The facts that the initial *p*-xylene permeance by the thicker (1000 nm) membrane is much higher than that of the five-times thinner (200 nm) membrane and the significant reduction of *p*-xylene permeance observed from the thicker (1000 nm) membrane are puzzling. Thus, the transient period is much longer for the thicker membrane. The research group of Tsaptasis also observed such a long transient period from their membranes.[35] The differences in microstructures of the membranes seem to play an important role and this is a subject of future studies.

The use of TEAOH and the 1:1 mixture of TPAOH and TEAOH instead of TPAOH gave similar results. However, the growth rate increased in the order of TPAOH > (TPAOH + TEAOH) > TEAOH (Figure S9). The mixture of tetrapropylammonium bromide (TPABr) and KOH can also be used instead of TPAOH (Figure S10). This is also a big advantage of gel-free secondary growth because TPABr is much cheaper than TPAOH (fifth requirement). When monolayers of *a*-oriented SL crystals [$(a\text{-SL})_m$] were placed on *p*-SiO_2 disks, continuous *a*-oriented SL films were produced on the substrates (see the Methods Section and Figure S11 in the Supporting Information). Interestingly, when a TPAOH-adsorbed $(a\text{-SL})_m/p\text{-SiO}_2$ and $(b\text{-SL})_m/p\text{-SiO}_2$ disks were placed together in a Teflon-lined autoclave, the corresponding perfectly *a*- or *b*-oriented SL films grew on each substrate. Thus, two different types of films could be grown simultaneously within an autoclave without interfering each other. This shows the scalability of the method for the growth of a large number of the same or different types of perfectly oriented zeolite films on various substrates in one batch, without wasting any chemicals, by using the minimum amounts of organic templates. This result also clearly shows that the orientation of the final film is governed by the orientation of the seed crystals.

There is no need to wash the films. This also greatly saves time and water and the extra step to dry the films. This method is also highly suitable for the growth of uniformly oriented films on large substrates because the pressure inside the reactor is much less than the cases of gel-based secondary growths owing to the use of much smaller amounts of water.

Overall, we report a novel film growth method named as "(preformed) gel-free secondary growth" to prepare uniformly *a*- and *b*-oriented SL films, which do not undergo crack-formation during removal of templates by calcination. Because this method does not use gels, the procedure is quite simple, saves time, does not waste chemicals, and even washing the films with water is not necessary, indicating that the method is highly economical and environment friendly, suitable for production of uniformly oriented SL films at industrial scale. This method is not limited to the growth of uniformly oriented SL films but can be applied to any desired zeolite films by finding proper methods to uniformly orient them on substrates. We believe our findings will trigger the development of economic and

environment-friendly methods for the preparation of various other types of zeolite films with perfectly uniform orientations.

Received: March 1, 2013
Published online: July 5, 2013

Keywords: membranes · mesoporous materials · silica · thin films

[1] J. O'Brien-Abraham, J. Y. S. Lin in *Zeolites in industrial separation and catalysis* (Ed.: S. Kulprathipanja), Wiley-VCH, Weinheim, **2010**, chap. 3, pp. 307 – 329.
[2] J. Caro, M. Noack in *Advances in nanoporous materials*, *Vol. 1* (Ed.: S. Ernst), Elsevier, Amsterdam, **2009**, chap. 1, pp. 1 – 96.
[3] J. Caro, M. Noack, *Microporous Mesoporous Mater.* **2008**, *115*, 215 – 233.
[4] J. Choi, H. K. Jeong, M. A. Snyder, J. A. Stoeger, R. I. Masel, M. Tsapatsis, *Science* **2009**, *325*, 590 – 593.
[5] J. Hedlund, F. Jareman, A. J. Bons, M. Anthonis, *J. Membr. Sci.* **2003**, *222*, 163 – 179.
[6] Z. P. Lai, M. Tsapatsis, J. R. Nicolich, *Adv. Funct. Mater.* **2004**, *14*, 716 – 729.
[7] C. J. Gump, V. A. Tuan, R. D. Noble, J. L. Falconer, *Ind. Eng. Chem. Res.* **2001**, *40*, 565 – 577.
[8] Z. P. Lai, G. Bonilla, I. Diaz, J. G. Nery, K. Sujaoti, M. A. Amat, E. Kokkoli, O. Terasaki, R. W. Thompson, M. Tsapatsis, D. G. Vlachos, *Science* **2003**, *300*, 456 – 460.
[9] M. A. Snyder, M. Tsapatsis, *Angew. Chem.* **2007**, *119*, 7704 – 7717; *Angew. Chem. Int. Ed.* **2007**, *46*, 7560 – 7573.
[10] H. H. Funke, A. M. Argo, J. L. Falconer, R. D. Noble, *Ind. Eng. Chem. Res.* **1997**, *36*, 137 – 143.
[11] J. O'Brien-Abraham, M. Kanezashi, Y. S. Lin, *J. Membr. Sci.* **2008**, *320*, 505 – 513.
[12] M. O. Daramola, A. J. Burger, M. Pera-Titus, A. Giroir-Fendler, L. Lorenzen, J.-A. Dalmon, *Sep. Sci. Technol.* **2010**, *45*, 21 – 27.
[13] H. Guo, G. Zhu, H. Li, X. Zou, X. Yin, W. Yang, S. Qiu, R. Xu, *Angew. Chem.* **2006**, *118*, 7211 – 7214; *Angew. Chem. Int. Ed.* **2006**, *45*, 7053 – 7056.
[14] K. Varoon et al., *Science* **2011**, *334*, 72 – 75.
[15] M. Tsapatsis, *Science* **2011**, *334*, 767 – 768.
[16] MFI is a framework type code assigned by the Structural Commission of the International Zeolite Association. Silicalite-1 and ZSM-5 belong to MFI. While ZSM-5 has aluminosilicate frameworks with varying Si/Al ratios, silicalite-1 has a pure silica framework.
[17] C. Baerlocher, W. M. Meier, D. H. Olson, *Atlas of zeolite framework types*, 5th ed., Elsevier, Amsterdam, **2001**, pp. 184 – 185.
[18] T. C. T. Pham, H. S. Kim, K. B. Yoon, *Science* **2011**, *334*, 1533 – 1538.
[19] W. Chaikittisilp, M. E. Davis, T. Okubo, *Chem. Mater.* **2007**, *19*, 4120 – 4122.
[20] L. H. Wee, L. Tosheva, L. Itani, V. Valtchev, A. M. Doyle, *J. Mater. Chem.* **2008**, *18*, 3563 – 3567.
[21] K. Hunt, C. M. Lew, M. Sun, Y. Yan, M. E. Davis, *Microporous Mesoporous Mater.* **2010**, *128*, 12 – 18.
[22] In fact, a gel is likely to form in situ during secondary growth. In this respect, the "gel-free growth" could more precisely be termed as "preformed gel-free growth".
[23] D. S. Bhachu, A. J. Smith, I. P. Parkin, A. J. Dent, G. Sankar, *J. Mater. Chem. A* **2013**, *1*, 1388 – 1393.
[24] J. S. Lee, J. H. Kim, Y. J. Lee, N. C. Jeong, K. B. Yoon, *Angew. Chem.* **2007**, *119*, 3147 – 3150; *Angew. Chem. Int. Ed.* **2007**, *46*, 3087 – 3090.
[25] K. B. Yoon, *Acc. Chem. Res.* **2007**, *40*, 29 – 40.
[26] H. S. Kim, S. M. Lee, K. Ha, C. Jung, Y.-J. Lee, Y. S. Chun, D. Kim, B. K. Rhee, K. B. Yoon, *J. Am. Chem. Soc.* **2004**, *126*, 673 – 682.
[27] H. S. Kim, K. W. Sohn, Y. Jeon, H. Min, D. Kim, K. B. Yoon, *Adv. Mater.* **2007**, *19*, 260 – 263.
[28] H. S. Kim, T. T. Pham, K. B. Yoon, *J. Am. Chem. Soc.* **2008**, *130*, 2134 – 2135.
[29] H. S. Kim, T. C. T. Pham, K. B. Yoon, *Chem. Commun.* **2012**, *48*, 4659 – 4673.
[30] C. M. Lew, R. Cai, Y. Yan, *Acc. Chem. Res.* **2010**, *43*, 210 – 219.
[31] Z. Li et al., *Angew. Chem.* **2006**, *118*, 6477 – 6480; *Angew. Chem. Int. Ed.* **2006**, *45*, 6329 – 6332.
[32] M. E. Davis, *Nature* **2002**, *417*, 813 – 821.
[33] T. Bein, *Chem. Mater.* **1992**, *8*, 1636 – 1653.
[34] G. Bonilla, M. Tsapatsis, D. G. Vlachos, G. Xomeritakis, *J. Membr. Sci.* **2001**, *182*, 103 – 109.
[35] G. Xomeritakis, S. Nair, M. Tsapatsis, *Microporous Mesoporous Mater.* **2000**, *38*, 61 – 73.